2E4-1

Proceedings of Symposium on Ultrasonic Electronics, Vol. 35 (2014) pp. 203-204
3-5 December, 2014

Vector contrast imaging of surface acoustic waves by local electric field probes

A. Habib[1], M. Pluta[2], U. Amjad[3], A. Shelke[4†‡], U. Pietsch[1], T. Kundu[3], R. Wannemacher[5], and W. Grill[2]

[1]Department of Solid State Physics, University of Siegen, Germany
[2]Institute of Experimental Physics II, University of Leipzig, Germany
[3]Department of Civil Engineering & Engineering Mechanics, University of Arizona, Tucson, USA
[4]Department of Civil Engineering, Indian Institute of Technology Guwahati, India
[5]Instituto Madrileño de Estudios Avanzados, Ciudad Universitaria de Cantoblanco, Madrid, Spain

1. Introduction

The generation and detection of surface acoustic waves (SAW) in piezoelectric crystals with the aid of digital (DT) or inter-digital transducers (IDT) has found widespread technological applications since the 1960s for signal processing and filtering applications [1]. There is currently renewed interest in SAW for sensor applications, in particular in view of biosensors [2]. SAW are surface guided acoustic waves, their amplitude drops towards the volume exponentially with a characteristic length of about one quarter of the wavelength. The velocity of acoustic waves and also SAW's is typically about five orders of magnitude smaller than that of electromagnetic waves. Due to these characteristics comb-shaped SAW transducers have typical periodicities in the mirometer size range for frequencies in the upper MHz to the lower GHz range (~15 GHz) [3].

A wide range of experimental SAW techniques were implemented to detect and visualize the surface acoustic wave field [4-9]. For an effective excitation of the surface acoustic waves, the conventional comb-shaped electrodes like DT or IDT placed on piezoelectric crystals are typically used. In view of imaging surface acoustic waves via electrical generation and detection the main problem with DT and IDT electrodes is that the operating frequencies, as well as the direction of propagation are determined by the transducer geometry.

In the presented work, such limitations are overcome by excitation with an approximate Dirac δ-function in the two spatial dimensions of the surface. We report visualization of SAW on a piezoelectric crystal by local electric field probes via Coulomb excitation and detection. The local probes are advantageous for wide band excitation and detection due to the absence of mechanical, geometrical and electrical resonances. The mass loading effect can be kept negligible, which is not the case for regular DTs and IDTs [10].

2. Experiments and Results

A similar experimental set-up employed for the observation of the transport of acoustic waves has been reported previously [11, 12]. A YZ-cut $LiNbO_3$ crystal of thickness 5 mm, both sides optically polished, was used for the experiments. The electrode for excitation and detection was fabricated from a 50 µm gold wire, wrapped around a bronze wire. Two 200 µm bronze wires were crossed in order to form a triangular lever holding the electrode to insure that it was in contact with the sample. The exciting electrode was positioned by a stepper motor driven 2D translation stage on the surface of the crystal.

It was scanned line by line over the imaged surface region during the experiment. The receiving electrode was placed at a fixed position on the same surface. It connects to a preamplifier in a metallic box acting as a Faraday cage. The minimum distance between the exciting and receiving probes is limited by the Faraday cage to about 0.5 mm. The scan area for the images displayed here has been set to 4×4 mm^2. An excitation burst with a carrier frequency of 89.9 MHz, gated to 220 ns (approximately, 20 oscillations) is cut from a continuous sine wave (CW) by an electronic switch. After amplification, the signal is delivered to the moveable local electric probe employed for excitation. Due to the piezoelectric effect the electrical signal is converted to ultrasonic oscillation and vice-versa. After amplification the detected signal is processed based on a quadrature detection scheme. For that purpose the signal is split and multiplied with two orthogonal reference signals (phase difference $\pi/2$). A low-pass filter removes the high-frequency components generated by multiplication. The low-pass-filtered signals are finally digitized by a two-channel transient recorder. The method presented visualizes the propagation of longitudinal bulk waves as well as SAW propagating along the surface of the piezoelectric $LiNbO_3$ crystal.

Figure 1 shows the magnitude of the transient signal obtained at the midpoint of a line scan, 0.5 mm away from receiving electrode in X direction.

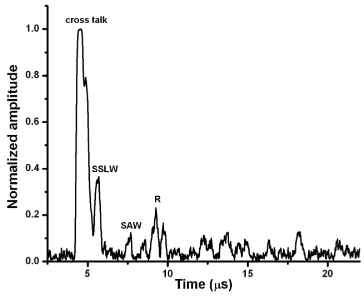

Fig. 1: Normalized magnitudes of the transient signal recorded with an electrode located on the same side of the crystal as the exciting electrode

Time gating applied to the acquired transient signals at different lateral positions yields the snapshots of the ultrasonic wave packages on the surface of the crystal. Figure 2 shows corresponding images demonstrating the observed transport properties of longitudinal bulk acoustic waves (L) and SAW (S) for propagation along the surface of a YZ-cut $LiNbO_3$ crystal. In the centre of the image between top and bottom the waves propagate in the direction of the crystal Z-axis. In figure 2 (left) the brightness reflects the magnitude of the measured electric signal of the observed waves as recorded on the crystal surface at a particular gating time. Fig. 2b, on the other hand displays the phase of the measured signal, wrapped around 2π.

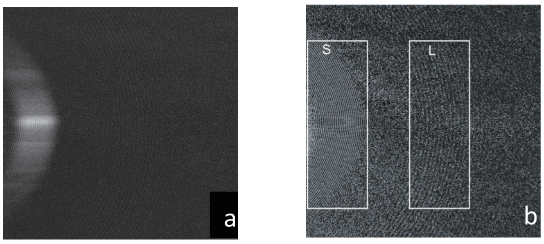

Fig. 2: Scanned wave fields of the surface skimming longitudinal waves (L) and surface acoustic waves (S). (a) Image in magnitude contrast and (b) phase contrast with full grey scale relating to 2π. The size of the images is 4 mm × 4 mm

The velocity of the longitudinal waves is about twice the SAW velocity. Therefore, the longitudinal polarized waves precede the observed SAW [13]. On the other hand, the intensity of the longitudinal waves drops faster than that of the surface guided SAW due to the different geometry. This feature is helpful for the identification of the observed wave patterns. The wavelengths are determined by the period of the regular structure of the visible waves. The measured velocity for propagation in the crystal Z-direction (group and phase velocity are degenerate in this case) of the surface skimming longitudinal waves is V_{SSLW}=7.45 (±0.1) km/s. The SAW velocity obtained from the measurement is V_{SAW}=3.56(±0.08) km/s, in good agreement with values given in the literature [14].

3. Conclusion

The Coulomb excitation and detection scheme is based on rather elementary effects and versatile because it is broadband and allows visualization of ultrasonic waves over large areas on arbitrary cuts of piezoelectric crystals. The scheme is independent of any lithography procedures as required for forming DT or IDT structures on the surface of a sample. The propagation of longitudinal polarized surface skimming bulk waves (SSLW) and SAW has been observed simultaneously by the developed technique. The technique is expected to find new applications in the field of generating and detecting SAW in piezoelectric materials.

Acknowledgement

The support of the European Union under the 7th Framework Program within AISHA II (Aircraft Integrated Structural Health Assessment II, EU-FP7-CP 212912) is gratefully acknowledged.

References

1. R. M. White, F.W. Voltmer, Appl. Phys. Lett, 7 (1965) 314
2. E. Howe, G. Harding, Biosens. Bioelectron, 15 (2000) 64
3. A. B. A. Dow, A. Ahmed, A. Bittner, C. Popov, U. Schmid, N.P. Kherani, Int. Ultrason. Symp.(2012), 968
4. R. W. Whatmore, P.A. Goddard, B.K. Tanner, G.F. Clark, Nature, 299 (1982) 44
5. H. Cerva, W. Graeff, phys. stat. sol. (a), 82 (1984) 35
6. T. Hesjedal, E. Chilla, H.J. Fröhlich, Surf. Interface Anal, 25 (1999) 569
7. R. E. Vines, S.I. Tamura, J.P. Wolfe, Phys. Rev. Lett., 75 (1995) 1873
8. D. V. Roshchupkin, M. Brunel, R. Tucoulou, E. Bigler, N.G. Sorokin, Appl. Phys. Lett, 64 (1994) 164.
9. W. A. Hamilton, M. Yethiraj, Phys. Rev. B, 59 (1999) 3388
10. D. V. Roshchupkin, T. Fournier, M. Brunel, O.A. Plotitsyna, N.G. Sorokin, Appl. Phys. Lett., 60 (1992)
11. A. Habib, E. Twerdowski, M.v. Buttlar, M. Pluta, M. Schmachtl, R. Wannemacher, W. Grill, Proc. SPIE, 6177 (2006) 383
12. A. Habib, A. Shelke, M. Pluta, U. Pietsch, T. Kundu, W. Grill, Int. congress on Ultrasonics, 1433 (2012) 247.
13. T. Makkonen, V.P. Plessky, W. Steichen, M. M. Salomaa, Appl. Phys Lett., 82 (2003) 3351
14. S.G. Joshi, B.D. Zaitsev, I.E. Kuznetsova, A.A. Teplykh, A. Pasachhe, Ultrasonics, 44 (2006) 787